A. M. Barnett

# Current Filaments in Semiconductors

**Abstract:** A current filament is a non-uniform radial distribution of current in the presence of a uniform electric field in a uniform sample. These filaments can have diameters in the 0.005 inch range. The current density at the center of the filament can be several orders of magnitude higher than the background current density in the rest of the sample. Filaments have been studied in devices exhibiting the current-controlled negative resistance associated with specific cases of two-carrier space-charge-limited current double injection. Electrons and holes are injected from opposite contacts into a semi-insulator in which the lifetime of carriers of one sign is much longer than the lifetime of carriers of the opposite sign. When forward biased this device exhibits a high-voltage, high-impedance ($10^8$ ohms) pre-breakdown region and a low-voltage, low-impedance (1 to $10^3$ ohms) post-breakdown region. In the post-breakdown region current increases at a nearly constant voltage followed by a high-current power-law region. Current filaments have been studied throughout the post-breakdown region by recording the recombination radiation observed through one of the injecting contacts. Experimental and analytical studies of current filaments in silicon at 77°K and GaAs at 300°K are reviewed.

## Introduction

The instability associated with current-controlled, or S-type, negative resistance in semiconductors can lead to a current filament. A current filament may be defined as a non-uniform radial distribution of current in a sample to which a uniform electric field is applied, as shown in Fig. 1.

Current-controlled negative resistance has been observed in many bulk effect and junction devices, including double-injection (two-carrier space-charge-limited current) devices,[1] avalanching p-i-n devices,[2] pnpn switches,[3] impurity impact ionization devices,[4] glass-type devices[5] and evaporated semiconductor devices.[6]

The first experimental report of current filaments was made during a study of impact ionization of shallow impurities in compensated germanium at 4.2°K.[7] Later, Ridley[8] postulated the existence of current filaments for the general case of current-controlled negative resistance in the dynamic negative resistance region. He did not, however, predict the existence of filaments beyond the negative resistance region. Muller and Guckel,[9] from conclusions based on a computer solution, described current filaments in the negative resistance region of avalanching p-i-n diodes.

Current filaments have been directly observed in double-injection devices by photographing the recombination radiation, which is transmitted through one of the injecting contacts. Such filaments have been observed in single-crystal silicon,[10] gallium arsenide,[11] zinc telluride,[12] gallium arsenide phosphide[13] and polycrystalline silicon.[6] There is also evidence for filamentary conduction in glass-type devices.[14]

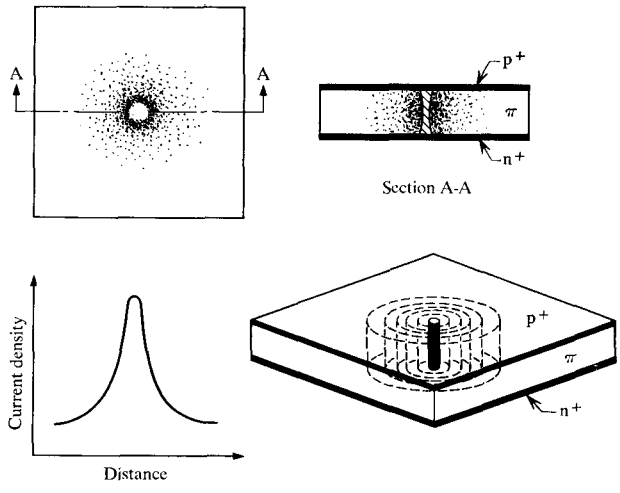


**Figure 1** Drawing of a current filament in a $p^+$-$\pi$-$n^+$ device.

This paper reviews the work that has been carried out on double-injection current filaments, emphasizing the similar observations in the direct-energy-gap semiconductor, gallium arsenide and the indirect-gap semiconductor, silicon.

The author is located at the Research & Development Center, General Electric Company, Schenectady, New York 12301.

## Double injection in semiconductors

When electrons and holes are injected into a high-resistivity semiconductor (semi-insulator), and the lifetime of the carriers of one sign is much longer than the lifetime of carriers of the opposite sign, devices that exhibit current-controlled negative resistance can result. Two-carrier space-charge-limited current filaments have been observed beyond the negative resistance region.

A voltage-current characteristic for a filamentary double-injection device is shown in Fig. 2 with the junction voltage drop subtracted. The solid line represents a model that is described later, and the points are experimental for semi-insulating silicon. At low levels, the characteristic is ohmic, followed by a region of space-charge-limited current that is dominated by injected minority carriers, with $I \propto V^2$. The voltage increases to a threshold voltage, $V_{th}$, and increases in current beyond this point mark the onset of negative resistance and two-carrier space-charge-limited current. Lampert[15] has described the negative resistance as being caused by the increase in lifetime of injected majority carriers due to the filling of traps. The voltage, then, decreases to a minimum voltage, $V_M$. The current now increases at nearly constant voltage until it reaches the region of a high-current power law, where $I \propto V^{1.5-2}$. Two-carrier space-charge-limited current filaments have been observed in the region where current increases at constant voltage[11] and in the high current power-law region.[10]

Lampert's theory[15] does not predict filaments, but it describes the observed negative resistance. Beyond the threshold voltage, Lampert's theory predicts a high-current square law region, $I \propto V^2$, based on a uniform post-breakdown current distribution. This uniform current distribution characteristic curve has been observed for *long* double-injection devices.[16]

In this paper, the experimental observations of current filaments occurring in the low-current region, where the current increases at constant voltage, and in the high-current power-law region, will be presented. A simplified theory that considers the current distribution of the filament, and the characteristic curve in the high-current power-law region, will also be described.

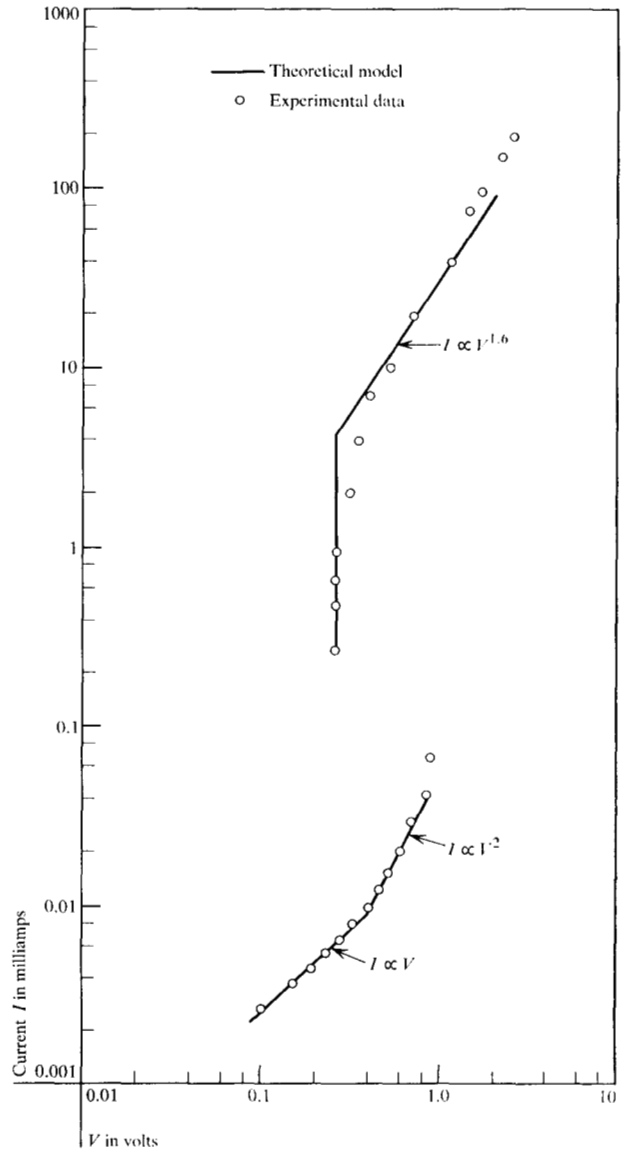


**Figure 2** Comparison of theoretical model and experimental results of the voltage-current characteristic curve for silicon device No. 25-1 (after Barnett and Milnes[10]).

## Experimental observations of current filaments

• *GaAs devices*

Good photographs of current filaments were taken for the direct band gap material, GaAs. These photographs were in the region where the current increases at nearly constant voltage.

A guard-ring geometry, which minimized pre-breakdown leakage current, was developed for the study of current filaments in semi-insulating GaAs.[17] It was found that surface leakage currents reduced the threshold voltage.* The devices were fabricated using $10^7$ ohm-cm oxygen-doped GaAs. The $n^+$ junction was formed by liquid-phase epitaxial growth. This injecting contact was 0.002 inches thick and 0.021 inches in diameter. A p-type guard ring was then placed around the $n^+$

* High pre-breakdown currents and low threshold voltages have been reported for semi-insulating GaAs at 77°K.[18] Low threshold voltages and, also, low currents were observed in the post-breakdown region, which are an order of magnitude lower than the values predicted by the non-filamentary Lampert theory. These values were used to develop a model for the negative resistance of p-i-n devices, based on the reabsorption of recombination radiation.[19] It is postulated that the reabsorption of recombination radiation of surface leakage current may cause a lowering of threshold voltage, but that the post-breakdown mechanism, for the most commonly reported GaAs p-i-n devices, is two-carrier space-charged-limited current filaments. A more detailed comparison of these two models appears in another work.[20]

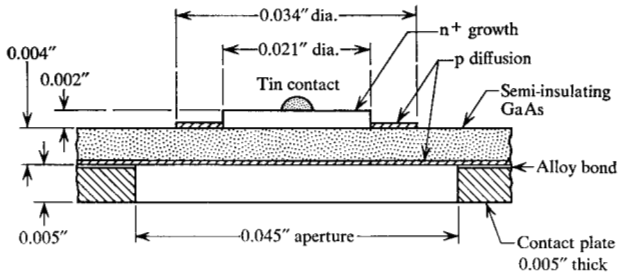


**Figure 3** Drawing of a GaAs p-i-n device with a guard ring to minimize surface leakage (after Barnett et al[17]).

**Figure 4** Photographs of GaAs current filaments at 6, 10, 15, 20 and 30 mA.

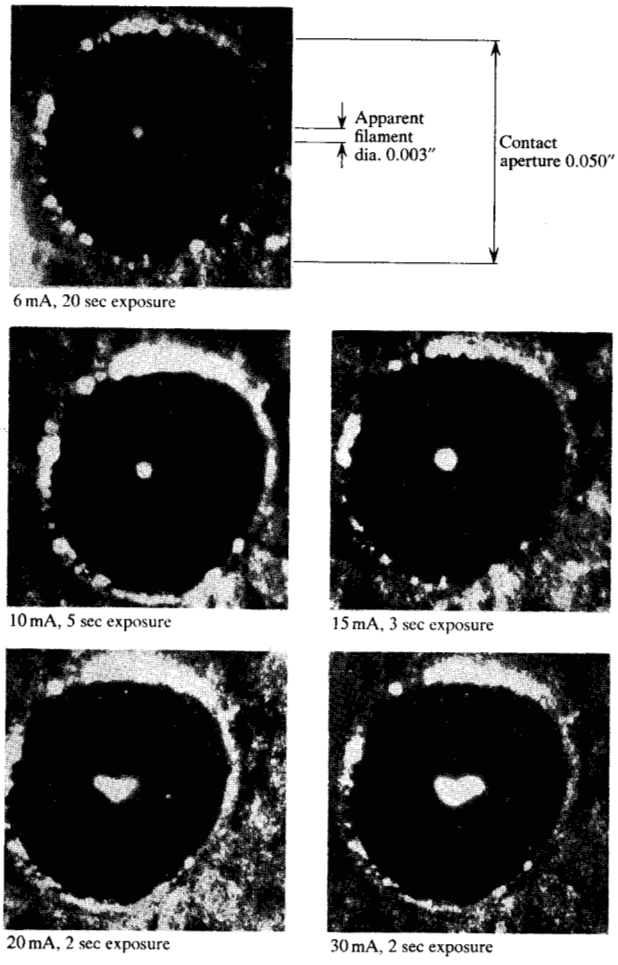


junction to minimize surface leakage current. The semi-insulating substrate was 0.004 inches thick and a 1-$\mu$m $p^+$ junction was diffused into the opposite face. The $p^+$ junction was alloyed to a gold-plated molybdenum contact with a 0.045-inch diameter aperture. A schematic drawing of the device is shown in Fig. 3.

For this device, the threshold voltage, $V_{TH}$, was 70 volts and the minimum voltage, $V_M$, was 6 volts. Photographs of single-current filaments (6, 10 and 15 mA) and multiple filaments (20 and 30 mA), which occurred in the low current region where the current increases at nearly constant voltage, are shown in Fig. 4. The voltage across the device, throughout this range of current, remained nearly constant at 6 to 7 volts, including the junction voltage.

• *Silicon devices*

The first direct observations of current filaments were reported in semi-insulating silicon at 77°K.[10] These observations in an indirect band gap material were in the high-current power-law region. The silicon was indium doped and had a thermal hole concentration, at 77°K, of $2 \times 10^{10}$ holes/cm$^3$, corresponding to a resistivity of approximately $10^4$ ohm-cm. An experimental technique, which permitted the direct observation of current filaments by collecting the recombination radiation through the $p^+$ junction, was developed. The p-i-n devices were stepped, with the semi-insulating region thicker near wire contact than elsewhere in the sample, as shown in Fig. 5. The purpose of the step geometry was to facilitate the nucleation of the filament in a region of the sample that is removed from the contact wires. Twelve devices with insulator lengths (in the thin region) between 140 and 220 microns were used. The other dimensions were approximately $1 \times 2$ mm. The $n^+$ junction was provided by a 10 micron phosphorous diffusion; the $p^+$ junction was provided by a 2 micron boron diffusion after the step was formed.

The device under study was suspended in liquid nitrogen with the $p^+$ junction facing a non-silvered section of the dewar. Radiation emerging from this window was focused onto the surface of an S1 image-converter tube. The image was derived from the 1.06 $\mu$m radiation. A simple lens was placed after the image converter to magnify the photographs. Exposure times ranged from minutes to hours.

The optical system was aligned by illuminating the device with a light pipe inserted in the dewar. The resultant background illumination system was used to obtain photographs of the device, which were then used to locate the position of the filament. Filamentary breakdown was observed in all of the devices that were 140 to 220 $\mu$m in length. Single filaments were observed in the high-current power-law region. Figure 6 shows photographs of single-current filaments, at 10 mA (0.5 V), 20 mA (0.7 V), and 40 mA (1.1 V), and multiple filaments at 80 mA (1.4 V) and 160 mA (2.2 V). This is the same device whose characteristics are shown in Fig. 2.

Photographs of this device, taken through a microscope and also through the image converter optical system,

are also shown in Fig. 6. The vertical line of light in these photographs represents reflections from the edge of the step. These photographs are of a rather low quality; therefore white circles have been added to indicate the approximate nucleation point of the first filament. These observed filaments are quite similar to the GaAs observations in Fig. 4.

An analysis of the current distribution within these filaments is presented in a later section.

• *Additional observations of current filaments*

Evidence of the direct observation of current filaments is found in at least four additional reports. Ing, Jensen and Stern[21] reported the emission of small spots of 8800 Å radiation through the zinc-diffused hole injecting contact in GaAs p-i-n devices. The $n^+$ junction was formed by alloying tin. They reported that they were unable to determine whether the geometrical configuration of the diode had any effect on the location and size of the region of emitted light.

Crowder, Morehead and Wagner[12] observed current filaments in their analysis of CdTe avalanche injection devices that exhibited negative resistance. Discussing the electroluminescence at 77°K, they noted that the light emission observed through the negative electrode comes from a small spot, so local current densities may be orders of magnitude higher than predicted by uniform current density considerations.

Current filaments were directly observed in evaporated silicon devices using an experimental technique similar to that described earlier. In this work negative resistance in evaporated silicon films was attributed to double injection.[6]

Gerhard and Jensen[13] observed negative resistance from $GaAs_xP_{1-x}$ with a p-i-n structure. They commented that the light emission appeared to result from a current filament.

• *Nature of the recombination radiation*

In these experiments the observed radiation is characteristic of conduction band to valence band (or impurity level) recombination, with a half-power bandwidth of several hundred angstroms. The electric field across the sample is quite low (as low as 10V/cm) and currents can be lower than one milliampere. Heating effects in GaAs devices were studied by noting the shift in peak wavelength. It was found that there were no changes in the peak wavelength below 50 mW. Thus, no heating effects occurred over a range of current of more than two orders of magnitude. One can conclude that these double-injection filaments are not caused by carrier or lattice heating effects, unlike the high-field, hot-carrier radiation observed by others during avalanche breakdown.[23]

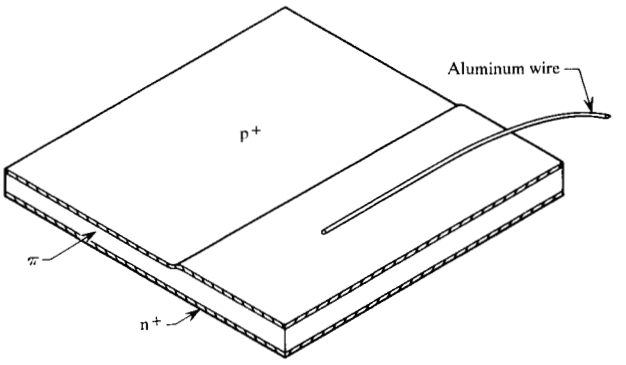


**Figure 5** Stepped geometry p-i-n device (after Barnett and Milnes[10]).

**Figure 6** Photographs of silicon current filaments at 10, 20, 40, 80 and 160 mA.

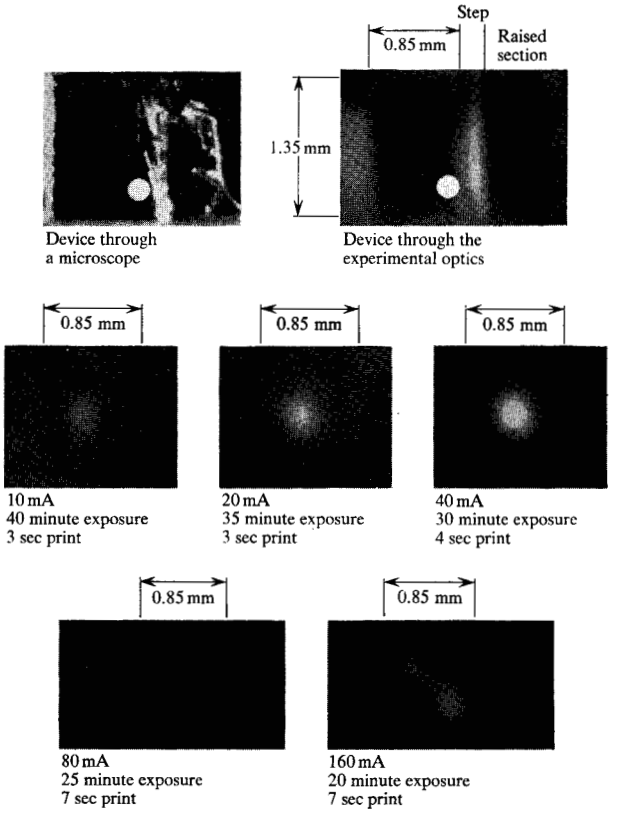


## Analysis of the silicon filaments

A model for the current distribution within the filament, based on the radial diffusion of carriers from a central core,[10] similar to the model for a gas plasma,[24] was developed. The carrier concentration at the center was based on Lampert's theory for double injection into an insulator. Consider the ambipolar diffusion constant, $D_a$,

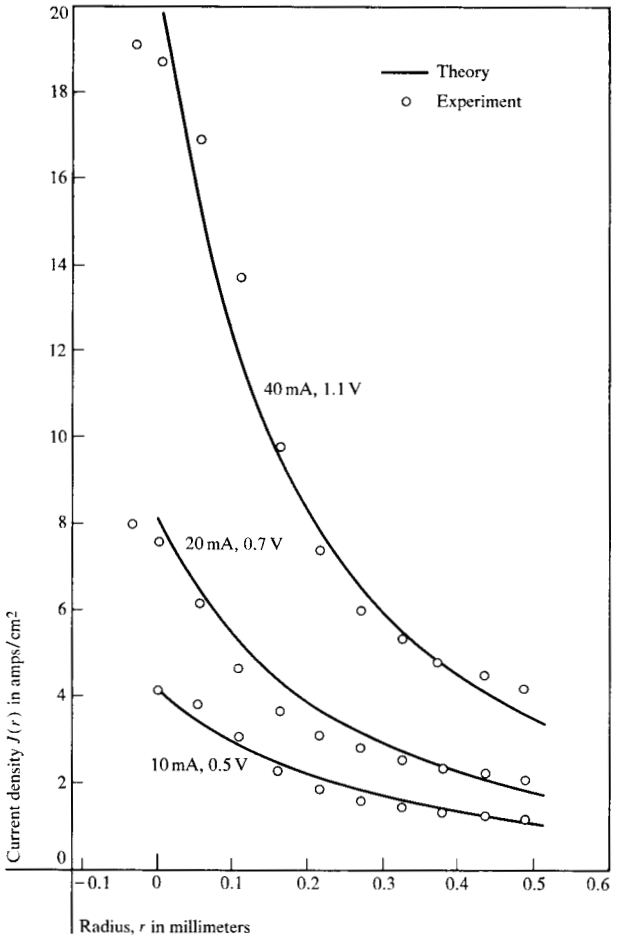


**Figure 7** Radial current distribution compared with the simplified filament equation for silicon device No. 25-1 at 10, 20 and 40 mA (after Barnett and Milnes[10]).

$$D_a \nabla^2 n = n/\tau \tag{1}$$

where $\tau$ is the carrier lifetime, and $n$ is the concentration of carriers of either sign. Due to the high concentration of injected carriers, bimolecular recombination is considered, $\tau = 1/(nC)$, where $C$ is the recombination constant, leading to

$$D_a \nabla^2 n = n^2 C. \tag{2}$$

The resultant non-linearities led to some mathematical simplification in order to develop a closed form solution.[10,20] The approximate solution for the variation of carrier concentration $n$, with radius $r$, is

$$n = n_0/[1 + (n_0 C/6D_a)^{\frac{1}{2}} r]^2. \tag{3}$$

The carrier concentration at the center, $n_0$, is defined by the Lampert conditions,

$$n_0 = [8\,\epsilon\mu_n\mu_p/eC\,(\mu_n + \mu_p)]^{\frac{1}{2}}(V/L^2), \tag{4}$$

where $V$ is the applied voltage, $L$ the insulator length, $\mu_n$ and $\mu_p$ the electron and hole mobilities, $\epsilon$ the dielectric constant, and $e$ the charge on a single carrier. By multiplying the carrier distribution by the electronic charge, the sum of the electron and hole mobilities and the average electric field, $V/L$, an expression is derived for the current density distribution.

$$J(r) = \frac{[8e\epsilon\mu_n\mu_p(\mu_n + \mu_p)/C]^{\frac{1}{2}}(V^2/L^3)}{\{1 + [(2\epsilon\mu_n\mu_p C/e(\mu_n + \mu_p)]^{\frac{1}{4}}(V/3D_a)^{\frac{1}{2}}(r/L)\}^2} \tag{5}$$

This equation is integrated to find the total current at an applied voltage. This model is applied to single filaments in the high-current power-law region for semi-insulating silicon.

• *Comparison of theory and experiment*

Single filaments were photographed in the high-current power-law region for semi-insulating silicon at 77°K, as shown in Fig. 6.

A linear relationship between current density $J$ and film density $D$ can be developed if all the constituent parts are linear. It has been shown,[10] for a set of experimental conditions, that the total current as a function of the light intensity is linear throughout a reasonable range; and that, for very low conditions, the film density is linear in response to the infrared light into the image converter. The film density was measured with a recording microphotometer, and was converted to current density by using a relationship of the form

$$J(r) = mD(r) + \text{constant}. \tag{6}$$

The solpe $m$ and the constant were determined from the 10-mA filament data, and used (with adjustments for exposure times) for the 20- and 40-mA filaments.

A comparison of the observed current distribution of the filaments with the theoretical variation of Eq. (5) is presented in Fig. 7. The 10-mA filament curve has been fitted at two points to determine the constants of Eq. (6). The curves computed from theory for the 20- and 40-mA filaments were derived without further fitting.

The filament, shown at 10, 20 and 40 mA in Fig. 7, is shown at 80 and 160 mA in Fig. 8, together with the characteristics of a secondary filament that appeared at these current levels. The primary filament is compared to the model, in Fig. 8, from 0 to 0.4 mm. The magnitude of the current density at the center of the secondary filament was determined experimentally and this value was applied to a form of Eq. (5) to determine the shape of the second filament (1.2 to 1.6 mm). The solid line between the peaks was drawn by using a linear combination of the two curves. At 80 mA the filaments are separated; at 160 mA the filaments appear to be joined.

The onset of the second filament may be accompanied by a small discontinuity in the current-voltage characteristic and/or by a change in the slope of the characteristic as shown in Fig. 2.

The agreement between theory and experiment under these conditions is satisfying.

• *Complete voltage-current characteristic*

The full characteristic curve has been described analytically by calculating a minimum current (assuming the minimum voltage and minimum carrier concentration at the filament center) and extending from this minimum current, at constant voltage, until the power-law curve is intersected. The advantage of this combined model is that it successfully predicts the shape of the post-breakdown current-voltage characteristic, which has been experimentally shown to be indigenous to double-injection filaments. A refined model is planned. Figure 2 shows the complete characteristic curve for the filamentary silicon device, Sample No. 25-1, compared with the model. Note that the onset of the second filament deviates from the single filament model. Similar voltage-current characteristics are observed for semi-insulating GaAs.[11]

The voltage-current characteristic shown in Fig. 2 has been observed for double-injection into semi-insulators, showing filamentary conduction in the post-breakdown region. An explanation of some of the boundary conditions for current filaments appears in another work.[20]

## Conclusions

Current filaments have been observed in many semiconductor materials. The current-controlled negative resistance characteristic can be reproducibly formed and studied. Monolithic arrays of GaAs filamentary devices, with as many as 100 devices on 0.050-inch centers, have been developed.[17] The reproducibility of the threshold and minimum voltage is shown for an 81-device array in Fig. 9. The uniformity of this array is a demonstration of the present degree of reproducibility of filamentary double-injection devices that can be attained.

The most important aspect of this study is, probably, the technique that was developed for analyzing recombination radiation viewed through a transparent injecting contact. The technique of analyzing emitted radiation through an injecting contact, using recombination radiation (either band-to-band or through trap centers) or heating effects (such as in avalanche breakdown), is a valuable tool, not only for the study of current filaments, but also for the study of injection phenomena in general.


## Acknowledgments

The direction of Professor A. G. Milnes of Carnegie–Mellon University, during the first study of space-charge-limited current filaments, has proved invaluable. In addition, my association with H. A. Jensen of the Electronics Laboratory of the General Electric Company has enhanced my understanding of the capabilities and limitations of related experiments.


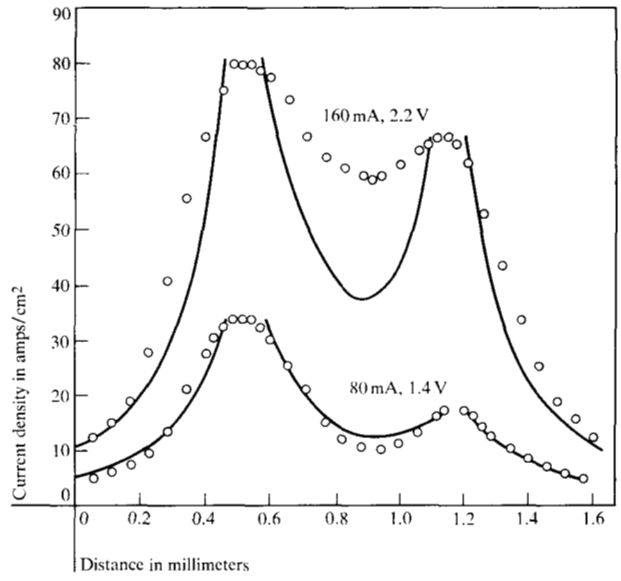


**Figure 8** Current density versus distance for the multiple filaments of silicon device No. 25-1 (after Barnett and Milnes[10]).

**Figure 9** Distribution of threshold and minimum voltages for LES-IC P49B with 81 devices (after Barnett et al[17]).

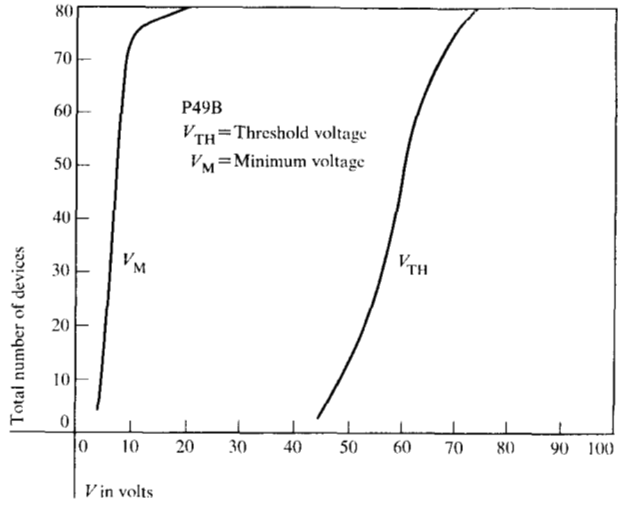


## References


1. W. W. Tyler, *Phys. Rev.* **96,** 226 (1954).
2. J. B. Gunn, *Proc. Phys. Soc. Lond. B,* **69,** 781 (1956).
3. J. L. Moll, M. Tannenbaum, J. M. Goldey and N. Holonyak, Jr., *Proc. I.R.E.* **44,** 1174 (1956).
4. A. L. McWhorter and R. H. Rediker, *Proc. IRE* **47,** 1207 (1959).

5. A. D. Pearson, W. R. Northover, J. F. Dewald, and W. F. Peck, Jr., *Advances in Glass Technology,* Plenum Press, New York 1962, p. 357.
6. M. Braunstein, A. I. Braunstein and R. Zuleeg, *Appl. Phys. Lett.* **10,** 313 (1967).
7. I. Melngailis and A. G. Milnes, *J. Appl. Phys.* **33,** 995 (1962).
8. B. K. Ridley, *Proc. Phys. Soc.* **82,** 954 (1964).
9. M. W. Muller and H. Guckel, *IEEE Trans. Elec. Dev.* **ED-15,** 560 (1968).
10. A. M. Barnett and A. G. Milnes, *J. Appl. Phys.* **37,** 4215 (1966).
11. A. M. Barnett and H. A. Jensen, *Appl. Phys. Lett.* **12,** 341 (1968).
12. B. L. Crowder, F. F. Morehead and P. R. Wagner, *Appl. Phys. Lett.* **8,** 148 (1966).
13. G. C. Gerhard and H. A. Jensen, *Appl. Phys. Lett.* **10,** 333 (1967).
14. A. D. Pearson, *IBM J. Res. Develop.* **13,** 510 (1969, this issue).
15. M. A. Lampert, *Phys. Rev.* **125,** 126 (1962).
16. J. W. Mayer, R. Baron and O. J. Marsh, *Appl. Phys. Lett.* **6,** 38 (1965).
17. A. M. Barnett, H. A. Jensen, V. F. Meikleham and H. C. Bowers, *1968 Int'l. Conf. on GaAs,* Inst. of Phys. and Phys. Soc., London (1968).
18. K. Weiser and R. S. Levitt, *J. Appl. Phys.* **35,** 2431 (1964).
19. W. P. Dumke, *Proc. 7th Int'l Conf. on Physics of Semiconductors,* Dunod, Paris (1964), p. 611.
20. A. M. Barnett, *Semiconductors and Semimetals, Vol. 6,* Academic Press, New York (to be published in 1969).
21. S. W. Ing, Jr., H. A. Jensen and B. Stern, *Appl. Phys. Lett.* **4,** 162 (1964).
22. A. G. Chynoweth and K. G. McKay, *Phys. Rev.* **102,** 369 (1956).
23. J. D. Cobine, *Gaseous Conductors,* McGraw-Hill Publishing Co. Inc., New York 1941, p. 233.

*Received April 18, 1969*